calculated iron d-orbital populations are in good agreement. However, one should keep in mind that the axial ligands are not identical in both studies (water versus THF) and that this may influence both the energy results and the electron distribution.

**Acknowledgment.** The calculations have been carried out on the CRAY computer of the CCVR (Palaiseau, France) through a grant of computer time from the Conseil Scientifique de Centre de Calcul Vectoriel pour la Recherche. We thank Professor Coppens for making his results available to us prior to publication.

**Registry No.** $FeP(H_2O)_2$, 122383-08-8.

Contribution from the Radiation Laboratory,
University of Notre Dame, Notre Dame, Indiana 46556

# Photochemical Reactivity of the Cluster $Mo_6Cl_{14}^{2-}$: Photosubstitution and Photoredox Processes

B. Kraut and G. Ferraudi*

*Received August 5, 1989*

Photoreversible ligand substitution and ligand oxidation reactions have been observed in UV photolyses of $Mo_6Cl_{14}^{2-}$ in acetonitrile. The photosubstitution of the ligand detected in $\lambda_{excit} > 300$ nm takes place in competition with population of the low-lying states associated with $Mo_6Cl_{14}^{2-}$ phosphorescence and leads to the formation of intermediates that can be scavenged by excess cluster, $Br^-$, or $I^-$. The photoredox reaction, investigated by continuous and flash photolyses, has been detected for irradiation at wavelengths of the high energy charge transfer bands, $\lambda_{excit} < 300$ nm. Similar oxidations of the ligand have been observed in experiments where the large concentration of low-lying excited states induces excited-state disproportionation and excited-state photolysis, respectively. The mechanism of ligand photosubstitution is discussed in terms of the photophysical and photochemical properties of $Mo_6Cl_{14}^{2-}$ in irradiations with low and high intensities.

## Introduction

The determination of the structure of molybdenum clusters, $Mo_6X_{14}^{2-}$, has shown that the nuclear configuration in these species consists of a nucleus of Mo atoms forming an octahedron while halide ions, X, occupy bridging and facial positions in a cubic array (I).[1-3] Metal-metal bonds in the complex have been described

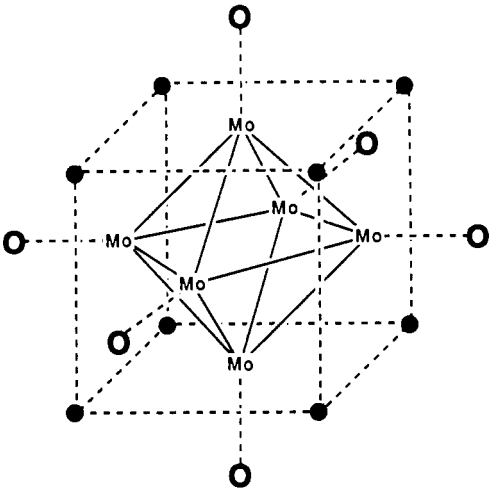


I

in terms of MO orbitals; the $t_{2g}$ HOMO constructed by overlapping $d_{xy}$ or $d_{yz}$, $d_{xz}$ orbitals and the $t_{1u}$ LUMO constructed by overlapping $d_{z^2}$ orbitals.[4,5] These calculations have provided some quantitative information about the position of the electronic states. Moreover, recent studies on the photochemistry of these compounds have demonstrated that the luminescence is associated with three closely spaced excited states, which are subjected to rapid thermal equilibration (eq 1-3).[5]

$$(T_{1u})Mo_6Cl_{14}^{2-} \xrightarrow{13\ \mu s} Mo_6Cl_{14}^{2-} + h\nu' \quad (1)$$

$$Mo_6Cl_{14}^{2-} \xrightarrow{h\nu} (E_u)Mo_6Cl_{14}^{2-} \xrightarrow{185\ \mu s} Mo_6Cl_{14}^{2-} + h\nu'' \quad (2)$$

$$(T_{2u})Mo_6Cl_{14}^{2-} \xrightarrow{370\ \mu s} Mo_6Cl_{14}^{2-} + h\nu''' \quad (3)$$

$$Mo_6Cl_{13}^{-} + Cl^- \longrightarrow \cdots \quad (4)$$

This mixture of states, namely 65.2% $T_{2u}$, 28.9% $E_u$, and 5.9% $T_{1u}$ relative Boltzmann populations at 298 K, gives rise to a long-lived phosphorescence, e.g. ca. 170 $\mu$s at 298 K in acetonitrile, which can be quenched by electron acceptors.[6-8] The ligand photosubstitution (eq 4) takes place by a path parallel to the formation of the photoemissive states and leads to the formation of reactive species that can be scavenged by halides or excess cluster.[9] In this work, the role of such intermediates in the photolysis of $Mo_6Cl_{14}^{2-}$ in $CH_3CN$ has been investigated under conditions that we have previously used in sequential biphotonic excitations, e.g. high laser intensities and/or high concentration of complex.[10,11] Also, new photoredox reactions induced in photolyses with $\lambda_{excit} < 250$ nm are reported here.

## Experimental Section

**Photochemical Procedures.** The apparatus used for flash photolysis and flash fluorescence experiments have been described elsewhere.[10-12] A flash lamp-pumped dye laser (Candela SLL-500 M) has been used for excitations at 440 nm. The output of the laser flash was varied by placing filters with appropriate optical densities in the light path. The light intensity was measured with a Scientech 365 power and energy meter. The solutions used for the flash experiments were deaerated with

(1) Brosset, C. *Ark. Kemi, Mineral. Geol.* **1945**, *20A*, No. 7.
(2) Brosset, C. *Ark. Kemi, Mineral. Geol.* **1947**, *25A*, No. 11.
(3) Vaughan, P. A. *Proc. Natl. Acad. Sci. U.S.A.* **1950**, *36*, 461.
(4) Zietlow, T. C.; Hopkins, M. D.; Gray, H. B. *J. Solid State Chem.* **1985**, *57*, 112.
(5) Saito, Y; Tanaka, H. K.; Sasaki, Y.; Azumi, T. *J. Phys. Chem.* **1985**, *89*, 4413.
(6) Maverick, A. W.; Gray, H. B. *J. Am. Chem. Soc.* **1981**, *103*, 1298.
(7) Maveric, A. W.; Najdzionek, J. S.; McKenzie, D.; Nocera, D. G.; Gray, H. B. *J. Am. Chem. Soc.* **1983**, *105*, 1878.
(8) Tanaka, H. K.; Sasaki, Y.; Saito, K. *Sci. Pap. Inst. Phys. Chem. Res. Jpn.* **1984**, *78*, 92.
(9) Kraut, B.; Ferraudi, G. Work in preparation.
(10) Van Vlierberge, B.; Ferraudi, G. *Inorg. Chem.* **1987**, *26*, 337.
(11) Van Vlierberge, B.; Ferraudi, G. *Inorg. Chem.* **1988**, *27*, 1386.
(12) Frink, M. E.; Geiger, D. K.; Ferraudi, G. *J. Phys. Chem.* **1986**, *90*, 1924.

0020-1669/89/1328-4578$01.50/0 © 1989 American Chemical Society

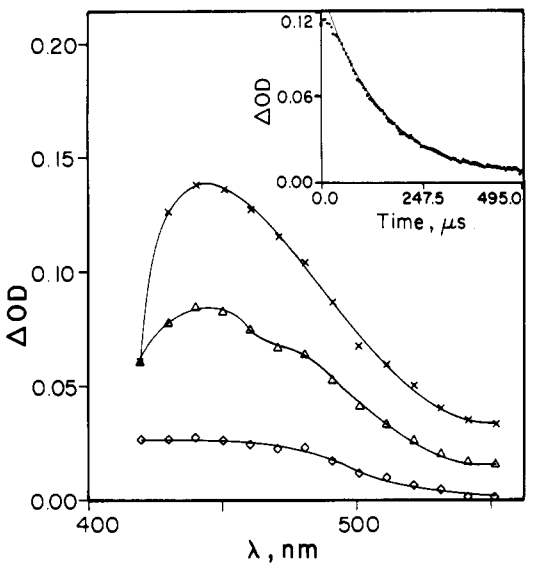


**Figure 1.** Transient spectra recorded in conventional flash photolyses ($\lambda_{excit} > 400$ nm) of $2.0 \times 10^{-4}$ M $Mo_6Cl_{14}^{2-}$ in deaerated acetonitrile with (×) 30-, (△) 150-, and (◇) 450-μs delays after the flash. The insert shows a typical trace for the decay of the 480-nm optical density. Each point in the spectra represents an average of 10 determinations with errors ΔOD of ±0.0003.

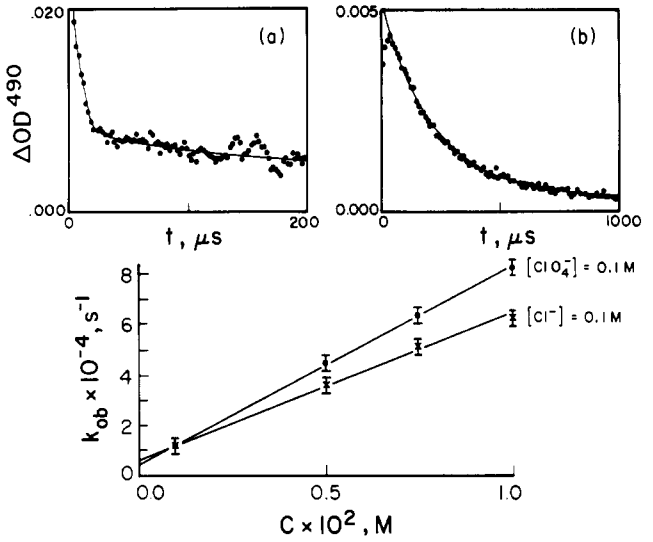


**Figure 2.** Dependence of the rate constant, $k_{ob}$, for the short-lived spectral decay on cluster concentration, $C$. The measurements were carried out with low-intensity flashes, i.e. $I_0 < 300$ (mJ/cm$^3$)/pulse and with an ionic strength, $I = 0.1$ M, adjusted with LiCl or $LiClO_4$ respectively. The insets show two traces, $\lambda_{ob} = 490$ nm, recorded in flash photolyses with concentrations of cluster, (a) $[Mo_6Cl_{14}^{2-}] = 10^{-2}$ M and (b) $[Mo_6Cl_{14}^{2-}] = 5.0 \times 10^{-4}$ M, that allow the observation of two steps or one step, respectively, in the decay of the transient spectra. In these traces, the solid lines are curve fittings described elsewhere in the text.

streams of ultrahigh-purity $N_2$ and refreshed after each irradiation. In conventional flash photolysis, two FP-8-100C (Xenon Corp.) flash lamps were used for irradiations.[12] Solutions were irradiated at preselected wavelengths by using appropriate cutoff filters. Continuous wave irradiations ($\lambda_{excit} > 360$ nm) were carried out with a 500-W high-pressure Hg–Xe lamp coupled with a high-intensity monochromator, collimating lenses, and IR filter. Relative values of the light intensity were determined with a photocell–microvoltmeter and absolute values were measured with tris(oxalato)ferrate(III).[13] A resonance Cd lamp was used for steady state excitations at $\lambda_{excit} = 229$ nm. In these 229-nm photolyses, the light intensity was measured with the hydrazoic acid actinometer.[14]

**Analytical Procedures.** Cyanogen was analyzed by gas chromatography after removal from irradiated solutions by vacuum distillation. In these experiments, the solutions of the complex were deaerated by three freeze–thaw cycles and irradiated for 4 h at 229 nm ($I_0 \sim 2.0 \times 10^{-6}$ einstein/L s). The barbituric acid–pyridine method was used for the determination of cyanide ion concentrations.[15] A modification of Sheldon's procedure was used for investigating the incorporation of $^{131}I^-$ in photolyses of $Mo_6Cl_{14}^{2-}$.[16] The product of the photolyses in the presence of $^{131}I^-$ and the excess Mo cluster was precipitated with 10% triphenylphosphonium chloride in concentrated HCl and washed several times with 10 cm$^3$ of the triphenylphosphonium chloride solution in order to remove free iodide. The radioactivity of the solid material was measured in an Ortec counter and correlated with the total amount of $I^-$ by means of previously constructed calibration curves.

**Materials.** The Mo complexes, $H_2Mo_6Cl_{14}$, $K_2Mo_6Cl_{14}$, $((C_4H_9)_4N)_2Mo_6Cl_{14}$, $((C_4H_9)_4N)_2Mo_6Cl_8I_6$, and $((C_4H_9)_4N)_2Mo_6Br_{14}$, were synthesized and purified by following literature procedures.[5,17-19] The purity of the compounds was established by comparing their absorption and emission spectra with those reported elsewhere.[6,7,19] Spectroquality acetonitrile, Aldrich Gold Label, was dried over molecular sieves for 24 h. The other chemicals were reagent grade and dried under vacuum before the preparation of the solutions.

## Results

**(1) Photochemical Reactions Induced by Irradiating $\lambda_{excit} > 300$ nm.** Flash photochemical irradiations of $Mo_6Cl_{14}^{2-}$ in deaerated $CH_3CN$ at $\lambda_{excit} > 400$ nm generates transient spectra (Figure 1) in a time shorter than 20 ps. Such spectra disappear with rates that are dependent on the concentration of complex and on the intensity of the flash. These observations indicate that the process leading to the decay of transient spectra is more complex than the single exponential decay of $T_{1u}$, $E_u$, and $T_{2u}$ under thermal equilibrium.[20] Therefore, the reaction mechanism has been studied under the range of experimental conditions reported below.

**(a) Intermediates in Flash Photolysis.** Least-squares curve fitting of traces recorded at $\lambda_{ob} = 500$ nm has shown that the decay rate of the transient spectra obeys first-order kinetics when irradiations are carried out with low-intensity flashes, e.g. in conventional flash photolysis or with a laser delivering less than or equal to 300 (mJ/cm$^3$)/pulse (Figure 2). In this low-intensity regime, the rate constants determined with diluted solutions, $[Mo_6Cl_{14}^{2-}] < 5.0\ 10^{-4}$ M, are in good agreement with the excited state relaxation rate constant, $k \sim 5.6 \times 10^3$ s$^{-1}$, measured in emission experiments by Gray et al.[6,7] However, time-resolved changes of the optical density in flash photolyses of solutions containing larger concentrations of the molybdenum complex, i.e. $10^{-3}$–$10^{-2}$ M, show two distinct processes whose rates obey first-order kinetics, (Figure 2). The slowest of the two processes exhibits a rate independent of the $Mo_6Cl_{14}^{2-}$ concentration with a rate constant, $k = 6.0 \times 10^3$ s$^{-1}$, that is very close to the one reported for the decay of the excited states. Measurements of the reaction rate for the fast process as a function of complex concentration and a constant ionic strength, $I = 0.1$ M in $LiClO_4$, reveal that the rate constant increases linearly with $Mo_6Cl_{14}^{2-}$ concentration (Figure 2). Although the rate of the fast process exhibited an inverse dependence on chloride ion concentration, the transient spectra recorded in flash photolyses of solutions with $5.0 \times 10^{-4}$ M $Mo_6Cl_{14}^{2-}$ in $10^{-2}$ M LiCl were the same determined with $LiClO_4$ instead of LiCl. These observations about the dependence of the absorbance decay rate on chloride and cluster concentrations can be combined in a single empirical rate law (eq 5) for two parallel processes. In eq 5, $A$ and $B$ are constants

$$\Delta OD = A \exp(-k_{es}t) + B \exp(-k_{ob}t) \quad (5)$$

proportional to the initial concentrations of excited state and intermediate respectively, $k_{es} \sim 6 \times 10^3$ s$^{-1}$ and $k_{ob} \sim 7 \times 10^5[Mo_6Cl_{14}^{2-}]/[Cl^-]$.

We have attempted the direct scavenging of $Mo_6Cl_{13}^-$ (eq 4) with high concentrations of species that are known to be good

(13) Hatchard, C. G.; Parker, C. A. *Proc. R. Soc. London, A* **1956**, *235*, 518.
(14) Shapira, D.; Treinin, A. *J. Phys. Chem.* **1973**, *77*, 1195.
(15) Fries, J. *Analyses of Trace Elements*: Merck: Darmstadt, FRG, 1971.
(16) Sheldon, J. C. *J. Chem. Soc.* **1960**, 3106.
(17) Sheldon, J. C. *J. Chem. Soc.* **1962**, 410.
(18) Hogue, R. D.; McCarley, R. E. *Inorg. Chem.* **1970**, *9*, 1354.
(19) Sheldon, J. C. *J. Chem. Soc.* **1960**, 1007.

(20) In the text, $^*Mo_6Cl_{14}^{2-}$ represents a given excited state or the mixture of them under thermal equilibrium.

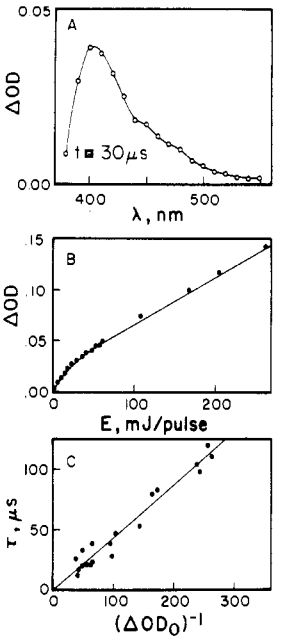


**Figure 3.** Flash photolysis of $5.0 \times 10^{-4}$ M $Mo_6Cl_{14}^{2-}$ under the regime of high-intensity flashes: (A) transient spectrum recorded 30 μs after 440-nm flash irradiations ($I_0 \sim 300$ (mL/cm³)/pulse; (B) nonlinear dependence of the 440-nm optical density change (1 μs after the flash) on the flash energy; (C) dependence of the half-life, $\tau$, of the transient spectra on the inverse of the 460-nm prompt optical density change, $\Delta OD_0$.

ligands, e.g. [$Br^-$] > 0.1 M, [triphenylphosphine] > 0.2 M, [diethylamine] > 0.1 M, respectively. These scavengers increase the rate of the transient spectra decay in accord with the scavenging of two intermediates: the emitting state and $Mo_6Cl_{13}^-$. It must be noted too that recovery of the unphotolized solution's spectrum after the flash irradiation of $Mo_6Cl_{14}^{2-}$ in 0.1 M $LiClO_4$, namely in the absence of any of the scavengers indicated above, is a slow process with about a 1 s lifetime.

In 440-nm flash photolysis with high intensities, i.e. more than 300 (mJ/cm³)/laser pulse and low concentrations of complex, i.e. [$Mo_6Cl_{14}^{2-}$] < $5.0 \times 10^{-4}$ M, the transient spectra recorded with delays of 1–30 μs after the flash exhibited an absorption band with $\lambda_{max}$ = 400 nm that was not observed with low-intensity irradiations; see above and Figure 3. Such transient spectra were, however, the same recorded in flash irradiations at wavelengths of the high-energy absorption bands, $\lambda_{excit}$ < 360 nm; see below. Since no clear growth of the 400-nm band has been observed—i.e., it grows during the irradiation, and the change in optical density at 440 nm increases with a nonlinear dependence on flash intensity (Figure 3b)—the generation of such a transient species has been associated with a sequential biphotonic excitation of $Mo_6Cl_{14}^{2-}$. Indeed, the empirical expression of ΔOD in terms of the flash intensity (eq 6) reveals opposite effects: the photogeneration of

$$\Delta OD \sim 1.6 \times 10^{-3} I_0 - 1.5 \times 10^{-6} I_0^2 \ldots \qquad I_0 \text{ in mJ/pulse} \qquad (6)$$

*$Mo_6Cl_{14}^{2-}$ and its photolysis with respective linear and higher order dependencies on $I_0$. In a time domain longer than 10 μs, the decay of the 460-nm optical density obeys second-order kinetics (Figure 3c) with $k_{an}/\epsilon = 1.9 \times 10^4$ cm $s^{-1}$, which is in accord with an annihilation reaction of the lowest lying excited state(s).

**(b) Irradiation Products.** In a time domain longer than several minutes, solutions ($10^{-4}$ M < [$Mo_6Cl_{14}^{2-}$] < $10^{-3}$ M, 0 < [$Cl^-$] < 0.01 M) irradiated ($\lambda_{excit}$ > 400 nm) with a large number of flashes or subject to continuous wave irradiations failed to show spectral changes that could be identified with the decomposition of the molybdenum complex. Spectral changes were observed, however, in continuous-wave photolyses of $10^{-3}$ M $Mo_6Cl_{14}^{2-}$ in 0.1 M LiBr. Such changes can be described as an hypsochromic shift of the spectrum that is in accord with the photosubstitution

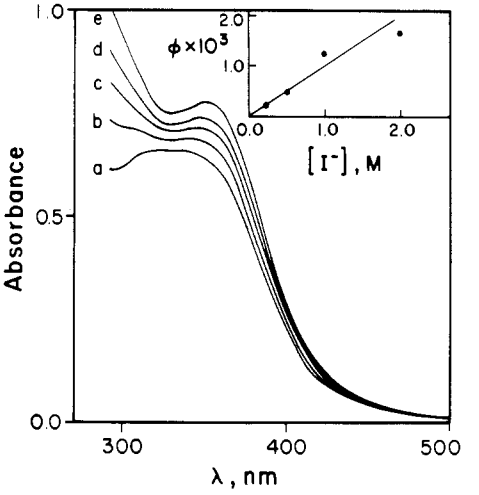


**Figure 4.** Spectral changes induced by 440-nm continuous-wave irradiations ($I_0 = 10^{-4}$ einstein/(L min)) of $10^{-3}$ M $Mo_6Cl_{14}^{2-}$ in 0.1 M $Br^-$ in 2 mm optical path: (a) 0 min; (b) 60 min; (c) 120 min; (d) 180 min; (e) 270 min. The inset shows the dependence of the quantum yield for $I^-$ incorporation to the cluster in 440-nm photolysis of $10^{-3}$ M $Mo_6Cl_{14}^{2-}$ in solutions containing given concentrations of $I^-$.

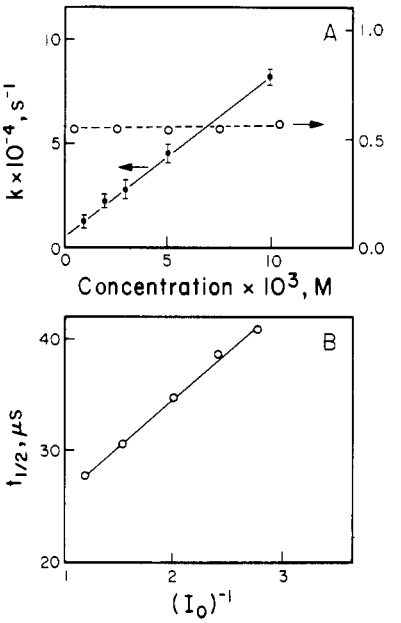


**Figure 5.** Kinetics of phosphorescence when $Mo_6Cl_{14}^{2-}$ is irradiated with (A) low-intensity and (B) high-intensity flashes. In part A, the independence of the emission rate constant (dashed line) on [$Mo_6Cl_{14}^{2-}$] is contrasted to the [$Mo_6Cl_{14}^{2-}$] dependence of the transient absorbance decay (solid line) in Figure 2. The dependence of the emission half-life on the inverse of the prompt emission intensity, $I_0$, is shown in part B. The intensity $I_0$ is given in arbitrary units.

of $Mo_6Cl_{14}^{2-}$ to form $Mo_6Cl_xBr_y^{2-}$ clusters with $x + y = 14$ (Figure 4). Although thermal ligand substitution reactions have been reported, blanks kept in the dark show little change in the time domain of the irradiations. Since the replacement of LiBr by LiI in the photochemical experiments led also to formation of mixed-ligand products, such a process has been followed by measuring the incorporation of $^{131}I^-$ into the molybdenum complex. Plots of the total concentration of $I^-$ incorporated in the Mo cluster vs irradiation time are linear with slopes that are proportional to the total $I^-$ concentration (Figure 4).

**(c) Kinetics of Emission.** Since the concentration-dependent rate for spectral decay in flash photolysis can be a consequence of self-quenching, we have investigated the rate of emission in flash fluorescence experiments ($\lambda_{excit}$ > 360 nm) carried out under the range of concentrations and low flash intensities indicated above. In these experiments (Figure 5), the time-resolved phosphorescence undergoes a single exponential decay with a half-life independent

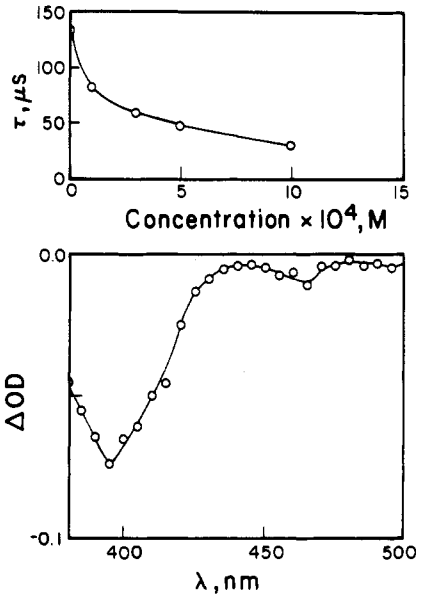


**Figure 6.** Quenching of the $Mo_6Cl_{14}^{2-}$ emission by Co(II). The dependence of the emission lifetime on the Co(II) concentration is shown at the top and the transient spectrum recorded for conventional flash photolysis of a solution containing $5.0 \times 10^{-3}$ M Co(II) is shown in the bottom. The data for the figures were collected in flash irradiations ($\lambda_{excit} \geq 400$ nm) of $2 \times 10^{-4}$ M $Mo_6Cl_{14}^{2-}$ with low-intensity flashes.

of the molybdenum concentration; i.e., the phosphorescence intensity, $I_p$, is given in eq 7, and must be combined with the excited

$$I_p = k_p[^*Mo_6Cl_{14}^{2-}] \quad (7)$$

state rate law (eq 8) in order to give a complete description of

$$\frac{\partial[^*Mo_6Cl_{14}^{2-}]}{\partial t} = -k_{es}[^*Mo_6Cl_{14}^{2-}] \quad (8)$$

the emission intensity. The half-life values measured at room temperature, $k_{es}^{-1} = \tau \sim 160$ μs, are in agreement with literature reports.[5-7]

The complex concentration independent lifetime of the emission stands in contrast with results from time-resolved absorption spectra (see section 1a) and demonstrate that the species involved in the absorption and emission of light react by parallel paths in the time domain of the phosphorescence.

Although the decay of the emission obeys a first-order rate law for excitations with low light intensities (Figure 5), departures from such kinetics are observed as the intensity of the excitation is increased to values comparable to those required for the detection of the 400-nm intermediate in flash photolysis. The dependence of the emission half-life on the exicted-state concentration shows that competitive processes with first- and second-order kinetics determine the rate of disappearance of the excited state (Figure 5b). In this high-intensity limit, eq 8 is not valid because one must add a term with a quadratic dependence on the excited-state concentration as is shown in eq 9. Such a quadratic term accounts for the annihilation of the excited state.

$$-\frac{\partial[^*Mo_6Cl_{14}^{2-}]}{\partial t} = k_{es}[^*Mo_6Cl_{14}^{2-}] + k_{an}[^*Mo_6Cl_{14}^{2-}]^2 \quad (9)$$

**(d) Quenching Experiments.** The $Co(CH_3CN)_6^{2+}$ quenching of the excited states was investigated by following the spectral changes in flash photolysis and by determining the rate of emission ($\lambda_{ob} = 805$ nm) in flash fluorescence, respectively. In emission experiments, the rate constant for the exponential decay of the light intensity increases linearly with Co(II) concentration. The slope determined from a plot of the rate constant vs the concentration of Co(II) gives a value, $k_q = 2.5 \times 10^8$ $M^{-1}$ $s^{-1}$, for the quenching rate constant. Moreover, flash photolysis, $\lambda_{excit} > 400$ nm, of $2 \times 10^{-4}$ M $Mo_6Cl_{14}^{2-}$ under conditions where the quenching of the emission by Co(II) is larger than 95%, i.e.

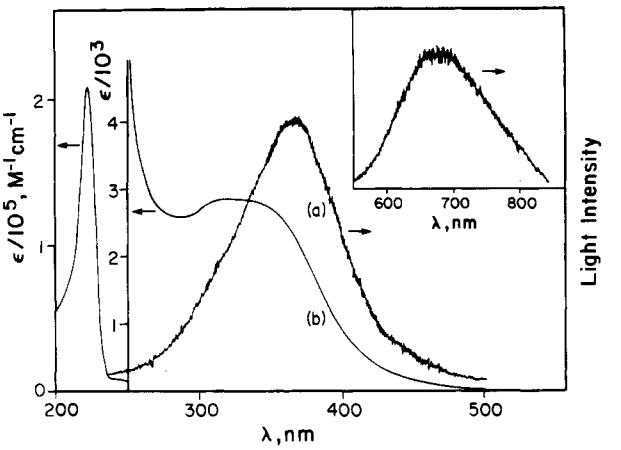


**Figure 7.** Comparison between spectra of $Mo_6Cl_{14}^{2-}$ at room temperature. The excitation spectrum (a) was determined by recording the emission intensity at 680 nm, i.e. the maximum in the absorption spectrum (inset). The emission spectrum was recorded for irradiations ($\lambda_{excit} = 360$ nm) of optically diluted solutions, $[Mo_6Cl_{14}^{2-}] = 3 \times 10^{-5}$ M. The absorption spectrum of the cluster is shown in curve b.

$[Co(II)] = 5 \times 10^{-3}$ M, induces a transient bleach instead of the transient spectra determined in the absence of the quencher (Figure 6). Since products from the oxidation and reduction of the molybdenum complex should be spectroscopically detectable in these experiments, the quenching by Co(II) can not be associated with an electron-transfer quenching of the emissive states. In this context, the bleach and recovery of the absorption spectrum must be regarded as a result of combined ligand substitution processes that regenerate the chloride cluster at the end of the reaction.

The $O_2$ quenching of the cluster's phosphorescence was investigated in acetonitrile solutions saturated with $O_2$ under 1 atm. The transient spectra recorded in flash photolysis of the oxygenated solution ($10^{-4}$ M $Mo_6Cl_{14}^{2-}$ and 0.1 M LiCl) were almost identical with the spectra recorded by quenching with $Co(CH_3CN)_6^{2+}$, see above. An excited-state quenching rate constant, $k_q \sim 10^8$ $M^{-1}$ $s^{-1}$, was measured from the decay rate of the transient spectra and the phosphorescence respectively. Since these experiments shown that the quenching reaction is completed in less than 2 μs, a transient, observed at $\lambda_m = 360$ nm with a half-life of about 100 μs, has been assigned to the reaction of $Mo_6Cl_{13}^-$ with excess cluster. Indeed, this result is in agreement with observations reported above (eq 5). Since $k_{es}$ in eq 5 must include the quencher, i.e. $k_{es} = 6 \times 10^3 + 10^8[O_2]$ $s^{-1}$, the first term vanishes at $t \leq 2$ μs while the second term ($k_{ob} \sim 7 \times 10^3$ $s^{-1}$) decays with a half-life of $\tau \sim 100$ μs.

**(2) Photochemical Reactions Induced by Irradiating $\lambda_{excit} < 250$ nm.** In order to establish the relationship between the electronic states populated by excitation at wavelengths of the high-energy bands, i.e. $\lambda_{excit} < 300$ nm, we have investigated the phosphorescence of the compound for excitations in this spectral region. The room-temperature excitation spectrum of $Mo_6Cl_{14}^{2-}$ in deaerated $CH_3CN$ was recorded by following the intensity of the phosphorescence at the maximum of the uncorrected emission spectrum, $\lambda_{em} = 680$ nm, for monochromatic excitations between 500 nm and 200 nm. Although the excitation spectrum partially overlaps with the low-energy end of the intense bands in the absorption spectrum (Figure 7), the yield of the phosphorescence decreases as the excitation progresses toward the high-energy end, i.e. $\lambda_{excit} < 320$ nm.

Continuous-wave irradiations of $Mo_6Cl_{14}^{2-}$ in deaerated $CH_3CN$ at 229 nm ($I_0 = 6.7 \times 10^{-6}$ einstein/($dm^3$ s)) induced minor spectral changes. These photolyses produced, however, trace amounts of cyanogen and $CN^-$ with yields of $\phi < 10^{-3}$. Intermediates associated with the formation of such products were investigated in flash photolyses where the concentration of cluster, $[Mo_6Cl_{14}^{2-}] < 10^{-4}$ M, limited the absorption of light by the solution to wavelengths of $\lambda < 300$ nm. Transient spectra recorded in such conditions disappear with mixed first- and second-order

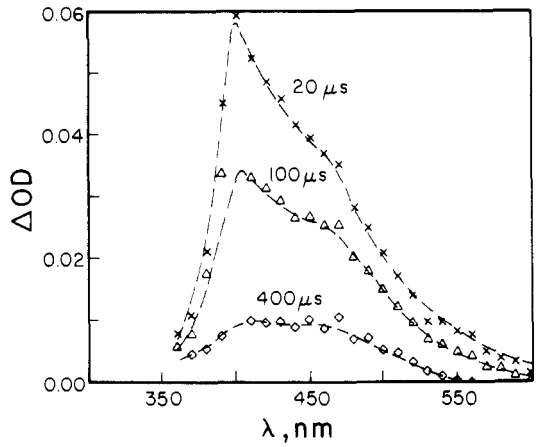


**Figure 8.** Transient spectra recorded for conventional flash photolysis (230 nm ≤ $\lambda_{excit}$ ≤ 300 nm) of $10^{-4}$ M $Mo_6Cl_{14}^{2-}$.

kinetics corresponding to half-lives, $t_{1/2} \sim 130$ μs, for flash-induced optical density changes, $\Delta OD_0 \sim 0.1$, (Figure 8). Moreover, the change of the 400-nm optical density after the flash and the rate of decay were independent of the water or $N_2O$ concentrations, i.e. for experiments with $[H_2O] \leq 2$ M and pH 1 with $HClO_4$, or ca. $10^{-2}$ M $N_2O$ respectively. These time-resolved observations are in accord with the photogeneration of $Cl_2^-$ in concentrations that are indicative of yields of radical ion larger than those reported above for cyanide and cyanogen.

## Discussion

The observations reported above show that the wavelength-dependent photochemistry of the $Mo_6Cl_{14}^{2-}$ cluster can be described in terms of photolabilization and photoredox processes. The characteristics of the mechanisms associated with such processes are discussed below.

**(a) Photolabilization Reactions ($\lambda_{excit} > 360$ nm).** In our study of the $Mo_6Cl_{14}^{2-}$ photochemistry under the regimen of excitation with low light intensities, a comparison of the results collected by time-resolved optical absorption and emission indicates that different transient phenomena are observed with these techniques. Although the kinetics of the emission can be directly associated with the relaxation of the excited states, this is not necessarily the case with the transient spectra where reaction intermediates, in addition to the excited and ground states, contribute with their absorptions to the differential absorption spectrum and its rate of disappearance. The nature of the reaction products and the failure to detect redox reactions in flash photolysis suggest that such intermediates are the products of photosubstitution reactions. In this regard, there must be at least one intermediate that can be rapidly scavenged by $Br^-$ or $I^-$ in order to form the mixed-ligand clusters. Moreover, the different dependences on $Mo_6Cl_{14}^{2-}$ concentration exhibited by the rates of emission and spectral decay must be interpreted in terms of scavenging of such intermediates by $Mo_6Cl_{14}^{2-}$ rather than self-quenching (eq. 10). In proposing

$$*Mo_6Cl_{14}^{2-} + Mo_6Cl_{14}^{2-} \rightarrow 2Mo_6Cl_{14}^{2-} \quad (10)$$

a mechanism for these processes, one must consider that the rate of spectral decay in the absence of excess chloride follows first-order kinetics while the rate of scavenging by $Mo_6Cl_{14}^{2-}$ exhibits an inverse dependence on chloride concentration. Such observations are in accord with a mechanism where equilibria involving the reaction intermediates and chloride ions occur in parallel to reactions where such intermediates are either or both transformed to products and scavenged by given reactants. For example, the results reported above can be rationalized in terms of the mechanism described in (eq 11–15). In the species $Mo_6Cl_{13}^-$ (eq 13–15), the displaced $Cl^-$ has been probably replaced by acetonitrile despite the general observation that acetonitrile is a poor ligand for the molybdenum clusters.[21,22] It is possible for such

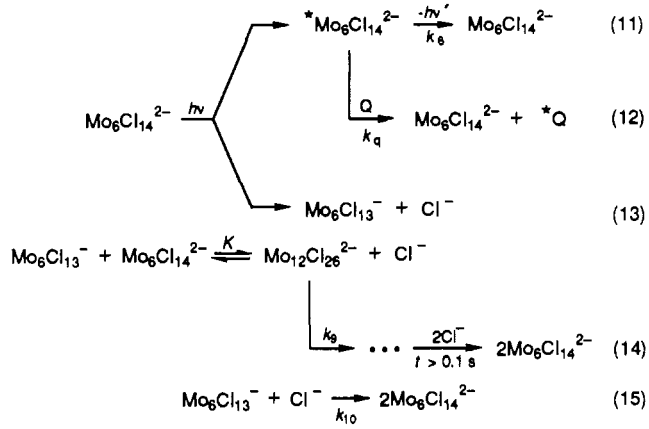


species to react with excess cluster or with $Cl^-$ (eq 14, 15). However, the first-order rate law for the transient spectra decay determined in flash photolysis with low concentrations of $Mo_6Cl_{14}^{2-}$ (Figure 2) has the same rate constant of the phosphorescence. This observation suggests that the rate of reaction of $Mo_6Cl_{13}^-$ with $Cl^-$ (eq 15) is smaller than the decay of the excited state (eq 11) in the absence of quencher Q (eq 12).[23]

The flash-photochemical observations, namely the rate of change of the optical density, can be expressed in a quantitative manner by using integrated rate equations (eq 16, 17), where $C_0$

$$C = C_0 \exp\{-k_{11}K([Mo_6Cl_{14}^{2-}]_0/[Cl^-]) \times (1/(1 + K[Cl^-]^{-1}[Mo_6Cl_{14}^{2-}]_0))t\}$$

$$C = [Mo_6Cl_{13}^-] + [Mo_{12}Cl_{26}^{2-}] \quad (16)$$

$$[*Mo_6Cl_{14}^{2-}] = [*Mo_6Cl_{14}^{2-}]_0 \exp(-k_{es}t)$$
$$k_{es} = k_{11} + k_q[Q] \quad (17)$$

and $[*Mo_6Cl_{14}^{2-}]_0$ are the product concentrations generated by the flash. In the derivation of the integrated rate law for $C$ (eq 16), we have assumed that the equilibration of $Mo_6Cl_{13}^-$ with $Mo_{12}Cl_{26}^{2-}$ (eq 14) is fast and use the equilibrium concentrations in eq 18 and 19.

$$[Mo_6Cl_{13}^-] = C\{1/(1 + K[Cl^-]^{-1}[Mo_6Cl_{14}^{2-}]_0)\} \quad (18)$$

$$[Mo_{12}Cl_{26}^{2-}] = C\{K[Cl^-]^{-1}[Mo_6Cl_{14}^{2-}]_0/(1 + K[Cl^-]^{-1}[Mo_6Cl_{14}^{2-}]_0)\} \quad (19)$$

The functional dependence on time (eq 21) of the flash-induced optical density change, ΔOD, has been found by making appropriate algebraic substitutions of eq 16–19 in eq 20, where $\epsilon_i$ with

$$OD = \epsilon_{gs}[Mo_6Cl_{14}^{2-}] + \epsilon_{es}[*Mo_6Cl_{14}^{2-}] + \epsilon_m[Mo_6Cl_{13}^-] + \epsilon_d[Mo_{12}Cl_{26}^{2-}] \quad (20)$$

i = gs, es, d, m, are the extinction coefficients of the various species at the wavelength of observation. Therefore, two terms whose

$$\Delta OD = \epsilon_{es}[*Mo_6Cl_{14}^{2-}]_0 \exp(-k_{es}t) + \{(\epsilon_m + \epsilon_d[Mo]/[Cl^-])/(1 + K[Mo]/[Cl^-])\}C_0 \exp(-k_{ob}t)$$

$$[Mo] = [Mo_6Cl_{14}^{2-}] + [*Mo_6Cl_{14}^{2-}] + [Mo_6Cl_{13}^-] + 2[Mo_{12}Cl_{26}^{2-}]$$

$$k_{ob} = k_{14}K([Mo_6Cl_{14}^{2-}]_0/[Cl^-]) \times (1/(1 + K[Cl^-]^{-1}[Mo_6Cl_{14}^{2-}]_0)) \quad (21)$$

respective weights are determined by various experimental conditions make contributions to ΔOD in eq 21. Under the approximation $1 > K[M_0]/[Cl^-]$ for the cluster concentrations used in our experiments, $k_{ob} \sim k_{14}K[M_0]/[Cl^-]$ and eq 21 can be recast in the form

(21) Kepert, D. L.; Vrieze, K. In *Halogen Chemistry*; Gutman, V., Ed.; Academic Press: New York, 1967, Vol. 3 pp 26–34.

(22) Ferguson, J. E. in *Halogen Chemistry*; Gutman, V., Ed.; Academic Press: New York, A. P., 1967; Vol. 3, pp 249–254.

(23) Cercone, E.; Camassei, F. D.; Giannini, I.; Sykora, J. *J. Photochem.* **1979**, *11*, 321.

$$\Delta OD = \Delta OD_0 \exp(-k_{ob}t) + \epsilon_{es}[^*Mo_6Cl_{14}^{2-}]_0(\exp(-k_{es}t) - \exp(-k_{ob}t)) \quad (22)$$

where $\Delta OD_0$ is the flash-induced optical density change at the beginning of the reaction. Equation 22 accounts for all our flash photochemical results in a microsecond time domain, e.g. the multiple decays of the flash-induced optical absorptions and the dependence of such decays on various experimental conditions, (Figure 2). For example, the curves for the fitting of the traces in Figure 2 were calculated by using eq 22 with appropriate experimental results. The curve in inset a was calculated with $\Delta OD_0 \sim 2 \times 10^{-2}$, $k_{ob} \sim 5 \times 10^4\ s^{-1}$, $\epsilon_{es}[^*Mo_6Cl_{14}^{2-}]_0 \sim 9 \times 10^{-3}$, and $k_{es} \sim 6 \times 10^3\ s^{-1}$. The curve for inset b was calculated with $\Delta OD_0 \sim 5.0 \times 10^{-3}$ and $k_{ob} \sim k_{es} \sim 4.0 \times 10^3\ s^{-1}$. It must be noted that the curve fitting of inset a gives $k_{14}K \sim 5 \times 10^5$ in good agreement with a value, $k_{14}K \sim 7 \times 10^5$, calculated from the slope of $k_{ob}$ vs $[Mo_6Cl_{14}^{2-}]$ in Figure 2.

Although the flash-photochemical transformations described above take place in a microsecond–millisecond time domain, on a longer time scale the observed spectral changes must be associated with reactions where $Mo_6Cl_{14}^{2-}$ is regenerated, e.g. transformations with $t > 0.1$ s in eq 14 and 15. Such a regeneration of the molybdenum cluster is in accord with results from continuous photolyses where no photolysis-induced spectral changes have been observed in the absence of added $I^-$ or $Br^-$.

**(b) Photoredox Reactivity.** The action spectrum recorded for excitations below 250 nm clearly shows that excited states populated in such irradiations cannot undergo efficient conversions to the low-lying manifold of emissive states. The appearance of photoredox reactivity in irradiations with $\lambda_{excit} = 229$ nm is therefore not surprising and can be related to a primary process involving the photooxidation of coordinated $Cl^-$ (eq 23–26).

$$Mo_6Cl_{14}^{2-} \xrightarrow[(\lambda_{excit} = 229\ nm)]{h\nu} \{Mo_6Cl_{13}^{2-}, Cl^\bullet\} \quad (23)$$

$$\{Mo_6Cl_{13}^{2-}, Cl^\bullet\} \rightarrow Mo_6Cl_{14}^{2-} \quad (24)$$

$$\{Mo_6Cl_{13}^{2-}, Cl^\bullet\} \rightarrow Mo_6Cl_{12}^{-} + 2Cl^- + \text{degradation products of } CH_3CN \quad (25)$$

$$\{Mo_6Cl_{13}^{2-}, Cl^\bullet\} \rightarrow Mo_6Cl_{12}^{-} + Cl_2^- \quad (26)$$

In eq 24–26, the bracketed species symbolizes a radical–ion pair that experiences competitive transformations leading to the regeneration of the parent cluster (eq 24), the decomposition of the solvent (eq 25), and the formation of the radical ion $Cl_2^-$ (eq 26). Inasmuch as the reactivity of $Cl^\bullet$ toward $CH_3CN$ is small, the dissociation in the halide ion radical (eq 26) and the regeneration of the $Mo_6Cl_{14}^{2-}$ (eq 24) must be the most important of the three reaction paths.[23] This proposition is in accord with the disparity of the product yields for the decomposition of the solvent and $Cl_2^-$ formation. The photoreversibility of the $Mo_6Cl_{14}^{2-}$ reaction in 229-nm irradiations must be attributed, therefore, to secondary reactions of the highly reactive $Mo_6Cl_{12}^-$ that regenerate the parent cluster.

**(c) High-Light-Intensity Photolysis ($\lambda_{excit} > 360$ nm).** Irradiation of $Mo_6Cl_{14}^{2-}$ at 440 nm with high-intensity flashes generates the same photoredox products of the photolyses as irradiation at $\lambda_{excit} < 250$ nm with low-intensity flashes. The mechanism of the product formation is clearly related to the high concentration of lowest lying excited states achieved in these experiments, concentrations leading to a significant absorption of the photolyzing light by the excited state and to its disappearance with second-order kinetics. In this regard, the reactions in eq 27 and 28 must be added to those describing the chemical

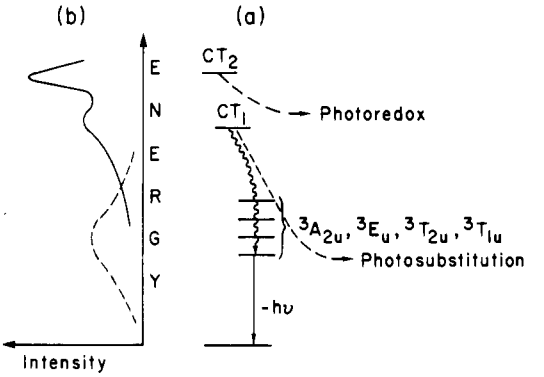


**Figure 9.** Tentative energy levels (a) of $Mo_6Cl_{14}^{2-}$ based on its photophysical and photochemial properties. For the sake of comparison, the absorption spectrum (solid line) and the emission spectrum (dashed line) are shown in part b.

$$^*Mo_6Cl_{14}^{2-} \xrightarrow{h\nu} \{Mo_6Cl_{13}^{2-}, Cl^\bullet\} \quad (27)$$

$$2^*Mo_6Cl_{14}^{2-} \rightarrow \{Mo_6Cl_{13}^{2-}, Cl^\bullet\} + Mo_6Cl_{14}^{2-} \quad (28)$$

transformations induced by low-light-intensity photolysis (eq 11–15, 24–26). It is possible that the secondary photolysis of the metal-centered excited state (eq 27) and its bimolecular annihilation reaction (eq 28) provide paths for the population of the same charge-transfer states that are photoactive in excitations at wavelengths shorter than 250 nm. If this is the case, it is intriguing that the reverse process, i.e. the charge transfer to the metal-centered states, does not compete with ligand oxidation and/or radiationless relaxation reactions according to the excitation spectrum of the Mo cluster (Figure 7).

## Conclusions

Since the absorption spectrum of the Mo cluster at low temperature shows weak absorption bands around 500–600 nm and MO calculations demonstrated the existence of excited states where the electronic density must be angularly displaced, i.e. with respect to the $^1A_{1g}$ ground state, the ligand photosubstitution and the phosphorescence can be associated with such metal-centered states. Some of these states are expected to exhibit significant distortions, i.e. tetragonal, with respect to the octahedral ground state, a condition that may favor ligand substitution. However, redox decompositions are characteristic of charge-transfer excited states where the electronic density is radially displaced with respect to the ground state. The possible involvement of such excited states is in accord with the assigment of some of the optical absorptions as charge-transfer transitions.[4] Communication between these two manifolds of excited states, i.e. metal-centered states and charge-transfer states, is poor. In this regard, the electronic levels in Figure 9 give an appropriate description of the photoprocesses observed in $Mo_6Cl_{14}^{2-}$.

**Acknowledgment.** The research described herein was supported by the Office of Basic Energy Sciences of the Department of Energy. This is Document No. NDRL-3119 from the Notre Dame Radiation Laboratory.

**Registry No.** $Mo_6Cl_{14}^{2-}$, 51364-21-7; $Co^{2+}$, 22541-53-3; $CH_3CN$, 75-05-8; LiBr, 7550-35-8; $O_2$, 7782-44-7; $Br^-$, 24959-67-9; $I^-$, 20461-54-5.